Available online at www.sciencedirect.com
ScienceDirect
Journal of Power Sources 184 (2008) 663–667
JOURNAL OF POWER SOURCES
www.elsevier.com/locate/jpowsour

Short communication

Preparation and electrochemical properties of ZnO/conductive-ceramic nanocomposite as anode material for Ni/Zn rechargeable battery

H. Huang, L. Zhang, W.K. Zhang *, Y.P. Gan, H. Shao

College of Chemical Engineering and Materials Science, Zhejiang University of Technology, Zone 6 Chaohui, Hangzhou 310032, Zhejiang, China

Received 28 November 2007; received in revised form 2 January 2008; accepted 2 January 2008
Available online 11 January 2008

Abstract

A novel ZnO/conductive-ceramic nanocomposite was prepared by a homogeneous precipitation between $Zn(NO_3)_2$ and $CO(NH_2)_2$ with conductive ceramic powders as the nucleation sites. The conductive ceramic powders contained zinc oxide, bismuth oxide, cobalt oxide and rare earth oxide, and the nominal chemical composition (mole fraction) was represented by $(ZnO)_{0.92}(Bi_2O_3)_{0.054}(Co_2O_3)_{0.025}(Nb_2O_5)_{0.00075}(Y_2O_3)_{0.00025}$. The phase composition and surface morphology of the as-synthesized materials were characterized by X-ray diffraction (XRD) and scanning electron microscopy (SEM). ZnO nanorods with the length of about 200 nm were dispersed homogeneously on the surface of the conductive ceramic, and identified as a well-defined single-phase hexagonal structure. The electrochemical properties of the ZnO/conductive-ceramic nanocomposite as anode material of Ni/Zn battery were investigated by charge/discharge cycling test, slow rate cyclic voltammetry (CV) and electrochemical impedance spectroscopy (EIS). Compared with pure nanosized ZnO, the ZnO/conductive-ceramic nanocomposite showed better cycling stability, higher discharge capacity and utilization ratio. The initial discharge capacity of ZnO/conductive-ceramic nanocomposite reached about 644 mAh g^{-1}. The discharge capacity hardly declined over 50 cycling tests, and the average utilization ratio could reach 99.5%. EIS revealed that the charge-transfer resistance was lower than that of pure nanosized ZnO.

Keywords: Nanosized ZnO; Ni/Zn secondary batteries; Conductive ceramic; Nanocomposite

1. Introduction

The nickel/zinc (Ni/Zn) battery is a promising power source for hybrid/electric vehicles and new portable devices. It delivers high specific energy (55–85 Wh kg^{-1}) and specific power (140–200 W kg^{-1}), and the nominal cell voltage (1.6 V) is 400 mV higher than that of Ni/Cd and Ni/MH batteries. Zinc oxide, commonly used as the anode material of Ni/Zn rechargeable battery, has attractive advantages of low toxicity, low cost and abundant resource. Nevertheless, its poor cycling characteristic limits widespread commercialization of Ni/Zn batteries [1,2]. The shape change of zinc electrode, zinc densification, passivation and dendrite growth that occur with increasing number of charge/discharge cycles are the main reasons for the short cycle life [3,4]. In the charge/discharge process, ZnO and Zn transformation relies on an intermediate product of soluble zincate ($K_2Zn(OH)_4$). The precipitation of soluble zincate leads to the formation of dendrites and Zn redistribution at the Zn electrode.

So far, many attempts have been made to reduce the problems of the Zn electrode shape change and dendrite growth, one approach is to add additives to either the electrode [5–10] or electrolyte [11–14]. Metal oxides or hydroxide, e.g., SnO_2 [5], Bi_2O_3 [6], CdO [7], PbO [8], $Ca(OH)_2$ [9,10], are convinced effective to improve cell lifetime and electrochemical performance of Ni/Zn batteries. These additives can reduce zincate concentration, provide an improved substrate for zinc electrodeposition, enhance electronic conductivity and current distribution [15–17]. The utilization of these additives is mainly physical mixture of ZnO and additives. However, this approach cannot provide homogeneous mixture and tight contact between the additives and ZnO particles, so that the efficiency of the additives is relatively low. In addition, some additives, due to their poor electronic conductivity, would increase the internal resis-

* Corresponding author. Tel.: +86 571 8832 0394; fax: +86 571 8832 0394.
E-mail address: msechem@zjut.edu.cn (W.K. Zhang).

0378-7753/$ – see front matter © 2008 Elsevier B.V. All rights reserved.
doi:10.1016/j.jpowsour.2008.01.004

tance of the battery and result in insufficient drainage of charges within active material during recharging, which handicaps the utilization of ZnO and cycling stability of Ni/Zn batteries.

In the present work, conductive ceramic powders are investigated as the additive of zinc anode for Ni/Zn rechargeable battery. The ZnO/conductive-ceramic nanocomposite is prepared by a homogeneous precipitation between $Zn(NO_3)_2$ and $CO(NH_2)_2$. The conductive ceramic powders as the nucleation sites of ZnO are added into the reactant solution to form homogeneous mixture, which can enhance the contact between the additive and ZnO particles and also increase the utilization efficiency of the additive. The electrochemical properties of the as-synthesized ZnO/conductive-ceramic nanocomposite are evaluated by charge/discharge cycling test, slow rate cyclic voltammetry (CV) and electrochemical impedance spectroscopy (EIS).

2. Experimental

2.1. Preparation of conductive ceramic powders

Accurately weighted powders of 92% ZnO, 5.4% Bi_2O_3, 2.5% Co_2O_3 and 0.075% Nb_2O_5 (mole fraction) were milled under ethanol in an agate vial using agate balls as a milling media. The operation was conducted in a QM-ISP2 type planetary high-energy ball mill (QM-ISP2) with a rotation speed of 400 rpm for 48 h. The ball-to-powder weight ratio was 20:1. The resulting slurry was dried at 75 °C and then calcined at 800 °C for 1 h. To eliminate large powder lumps, the as-calcined powder mixture was milled again for 48 h under the same conditions. Then the obtained powder was mixed with $Y(NO_3)_3$ sol completely. After solvent evaporation, the powder was heated to 1200 °C with a heating rate of 5 °C min^{-1} in air and maintained at this temperature for 2 h. After the natural cooling to the room temperature, the as-sintered powder was ball milled into fine particles. The nominal chemical composition of the conductive ceramic powders was represented by $(ZnO)_{0.92}(Bi_2O_3)_{0.054}(Co_2O_3)_{0.025}(Nb_2O_5)_{0.00075}(Y_2O_3)_{0.00025}$.

2.2. Preparation and characterization of ZnO/conductive-ceramic nanocomposite

The ZnO/conductive-ceramic nanocomposite was prepared using homogeneous precipitation process with $Zn(NO_3)_2$ and $CO(NH_2)_2$ as the reactant, by adjusting the mixing ration $Zn(NO_3)_2$:$CO(NH_2)_2$ = 1:3. The conductive ceramic powders in the given ratio (the content of conductive ceramic is about 14 wt.%) was used as the nucleation sites. In order to improve the dispersion of conductive ceramic powders, the solution was treated by ultrasonic vibration for 10 min. Then the reaction was carried out at 92 °C for 4 h with constant stirring. The obtained precursor product was filtered, washed copiously with distilled water and then calcined at 500 °C for 3 h. The phases presented in the nanocomposite were identified by powder X-ray diffraction (Philips PC-APD with Cu Kα radiation). The surface morphology of the powder was observed by scanning electron microscope (SEM, HITACHI S-4700 Π) and transmission electron microscopy (TEM). Pure nanosized ZnO was also fabricated by the above process with the same regents of $Zn(NO_3)_2$ and $CO(NH_2)_2$.

2.3. Preparation of zinc electrode and electrochemical tests

Zinc electrode was prepared by incorporating slurries containing the as-prepared ZnO/conductive-ceramic nanocomposite, Bi_2O_3, acetylene black, CMC and PTFE to a Ni foam substrate (2 cm × 2 cm in size). The weight ratio of active material, Bi_2O_3, acetylene black, CMC (3%) and PTFE (60%) was 100:5:0.5:18.75:6.25. Pasted zinc electrode was dried at 50 °C and pressed to a thickness of 0.3 mm at 10 MPa. For comparison, similar zinc electrodes with pure nanosized ZnO were also fabricated. A solution of 4 M KOH, 1.6 M K_2BO_3, 0.9 M KF and 0.1 M LiOH, saturated with ZnO was used as the electrolyte. Multi-layer cellulose triacetate microporous membranes were used as the separator to retard Zn dendrite penetration and prevent the electrodes from shorting. The Zn electrode and $Ni(OH)_2$ electrode were assembled into a cell and placed in a simple cell container made of perspex. The capacity of the $Ni(OH)_2$ electrode was far more than that of the Zn electrode.

The charge/discharge cycling tests were performed using a BS-9390 battery tester (Guangzhou Qingtian) at room temperature (25 ± 2 °C). The cells were charged at 0.2 C for 5.5 h, and then discharged at 0.2 C down to 1.2 V cut-off. The CV experiments were carried out on an electrochemical workstation (CHI660B) with a scanning rate of 0.1 mV s^{-1}. A three electrode cell was used with a Hg/HgO electrode as the reference electrode, a $Ni(OH)_2$ electrode as the counter electrode and a pasted zinc electrode as the working electrode. The electrochemical impedance spectroscope (EIS) measurements were performed on CHI660B in the frequency range between 0.01 Hz and 100 KHz. The amplitude of AC signal was 5 mV.

3. Results and discussion

Fig. 1(a) shows the XRD pattern of conductive ceramic powders. The main diffraction peaks are attributed to ZnO and the others are Bi_2O_3 and $YNbO_4$ phase. Fig. 1(b) shows the XRD patterns of ZnO/conductive-ceramic nanocomposite and pure ZnO powder prepared by precipitation method. The diffraction peaks of both samples can be indexed as a single and well-defined ZnO phase with hexagonal structure. No obvious peaks of Bi_2O_3 and $YNbO_4$ phase originating from the conductive ceramic are detected in the nanocomposite because of the low amount of addition.

Fig. 2 shows the SEM images of conductive ceramic and ZnO/conductive-ceramic nanocomposite, respectively. From Fig. 2(a), it is observed that the conductive ceramic particles have irregular surface morphology, and the particle sizes range from 0.2 to 2.0 μm. For the ZnO/conductive-ceramic nanocomposite, a lot of nanorods with the length of about 200 nm are uniformly dispersed, as shown in Fig. 2(b). EDS analysis confirms that these nanorods are ZnO. The conductive ceramic powders as the nucleation sites are embedded into ZnO through the surface precipitation process. For comparison, the TEM image of pure

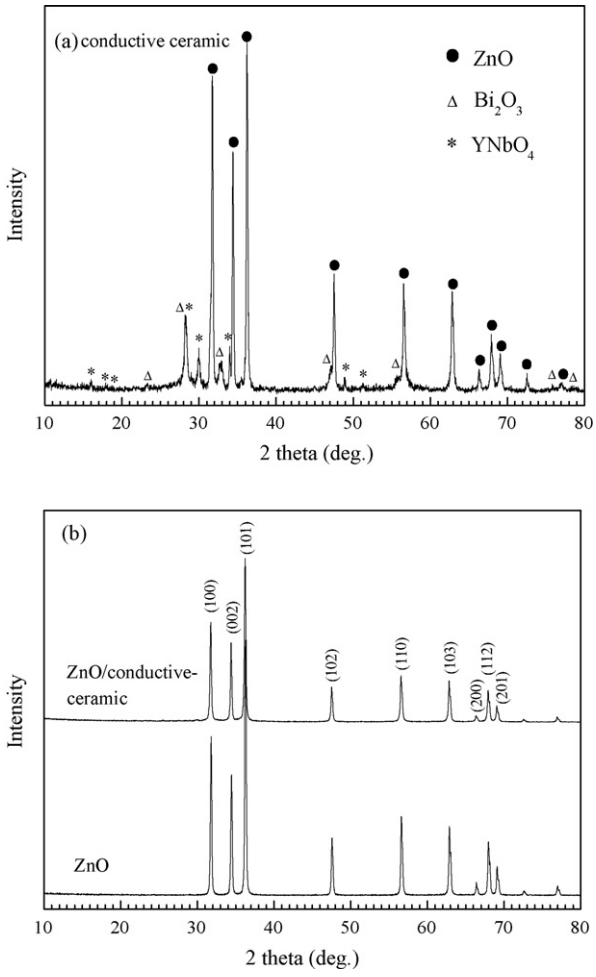

Fig. 1. XRD patterns of (a) conductive ceramic and (b) ZnO/conductive-ceramic nanocomposite and pure nanosized ZnO.

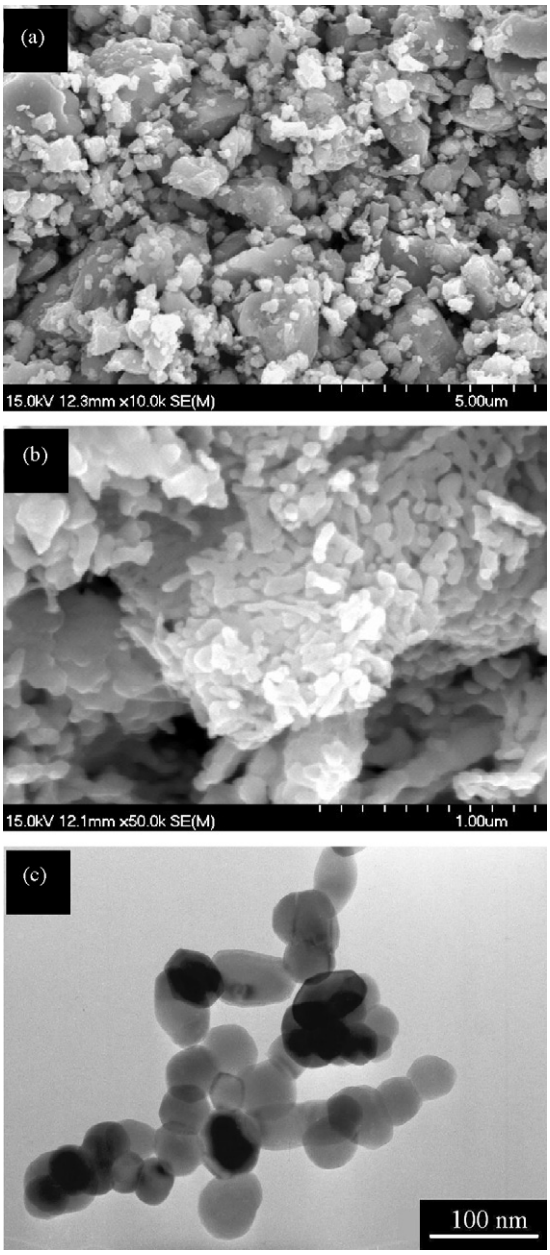

Fig. 2. Surface morphology of (a) conductive ceramic, (b) ZnO/conductive-ceramic nanocomposite and (c) pure nanosized ZnO.

ZnO prepared by precipitation method is shown in Fig. 2(c). The nanosized ZnO powders are well-crystallized hexagonal prism, and the particle sizes are about 30–80 nm.

Fig. 3 illustrates the electrochemical cycle behaviors of the electrodes with pure nanosized ZnO and ZnO/conductive-ceramic nanocomposite. The initial discharge capacity of pure ZnO is about 513 mAh g^{-1}, however, it suffers from rapid capacity fade after several cycles. At the 50th cycle, the discharge capacity decreases to 268 mAh g^{-1} with a retention of 52.2%. In comparison with pure ZnO, the initial discharge capacity of ZnO/conductive-ceramic nanocomposite is significantly improved, reaching about 644 mAh g^{-1} (the calculation of discharge capacity excludes the mass of conductive ceramic). The discharge capacity hardly declines over 50 cycling tests, the average utilization ratio (average discharge capacity/theoretic capacity of 659 mAh g^{-1}) could reach 99.5%, and the electrode has no obvious weight loss after cycling tests.

The typical charge/discharge curves of Ni/Zn batteries tested at the 12th cycle are displayed in Fig. 4. The ZnO/conductive-ceramic nanocomposite compares favorably with pure ZnO in terms of charge plateau voltage, discharge plateau voltage and specific capacity. For the ZnO/conductive-ceramic nanocomposite, the low charge plateau voltage conduces to the suppression of H_2 formation and the improvement of charge efficiency. The narrow charge/discharge voltage range and the high discharge value are evidence for its good electrochemical performance.

The high capacity retention and good electrochemical performance can be ascribed to the following reasons. The conductive ceramic powders are used to form a highly conductive network, which helps to improve the electrical contact between ZnO particles and diminish the polarization of the electrode. Another reason is that during the course of the preparation of the nanocomposite, the conductive ceramic as the nucleation sites would lead to homogeneous precipitation of ZnO particles on their surface, which can increase the space between ZnO particles and the actual reaction surface area of active mate-

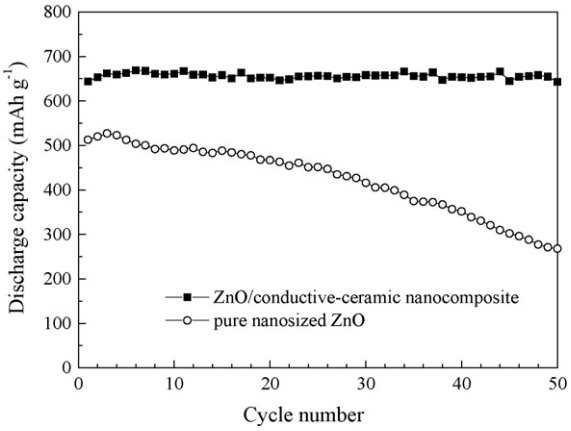

Fig. 3. Electrochemical cycle behaviors of the electrodes with the pure nanosized ZnO and ZnO/conductive-ceramic nanocomposite, respectively.

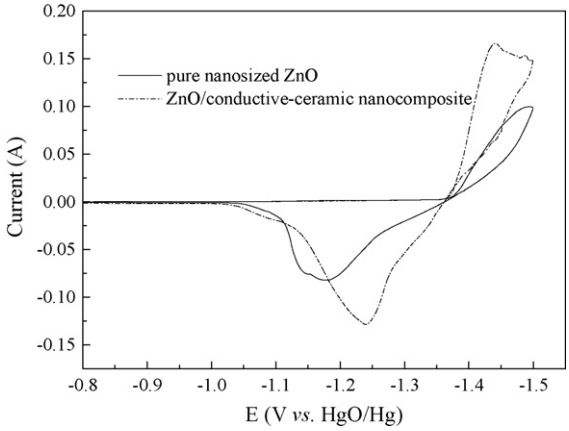

Fig. 5. Cyclic voltammograms of the electrodes with the pure nanosized ZnO and ZnO/conductive-ceramic nanocomposite, respectively.

rial. During charge/discharge processes, conductive ceramic will become stable growth center of the electrodeposits. It has been proposed and widely accepted that the shape and orientation of the electrodeposits are completely depended on the characteristics of the growth center [18]. Since the conductive ceramic is stable and not dissolved in the electrolyte, the initial shape and size of nanosized ZnO are kept. Therefore, the shape change, densification of Zn electrode and dendrites are alleviated. The activity of ZnO is retained and the utilization of active material is also increased.

To further investigate the effects of the conductive ceramic on the electrochemical reactions of ZnO electrode, cyclic voltammetry was conducted in the potential region from -0.8 to -1.5 V, at a scanning rate of $0.1\,\mathrm{mV\,s^{-1}}$. Fig. 5 illustrates the cyclic voltammograms of the electrodes with pure nanosized ZnO and ZnO/conductive-ceramic nanocomposite. Both electrodes show a pair of distinctive current peaks, which constitute the basis for the zinc oxide electrode in rechargeable battery application. The overall electrode reaction can be described as $Zn + 4OH^- \leftrightarrow Zn(OH)_4^{2-} + 2e^-$ and $Zn(OH)_4^{2-} \leftrightarrow ZnO + 2OH^- + H_2O$ [19]. From Fig. 5, the cathodic and the anodic peak currents of the ZnO/conductive-ceramic electrode are much higher than those of pure nanosized ZnO electrode, which indicates that the conductive ceramic added to ZnO can improve the electrochemical reactivity of Zn electrode. The reversibility of the electrode reaction can be measure by the difference ($E_O - E_R$) between the oxidation peak (E_O) and the reduction peak (E_R). It is clear that the reversibility for the Zn electrode is significantly improved by the addition of conductive ceramic powders.

Fig. 6 shows the impedance plots of the electrodes with pure nanosized ZnO and ZnO/conductive-ceramic nanocomposite at 100% state-of-charging (SOC). For both electrodes, the Nyquist plots are characteristics of one capacitive semicircular loop in the high-frequency range and one sloping straight line in the low-frequency range. The high-frequency capacitive semicircular loop can be considered as due to the charge-transfer resistance in parallel with the double layer capacitance, and the low-frequency straight line reflects the diffusion of zincate in the ZnO electrode. The equivalent circuit is presented in Fig. 7, where Q_{dl} is the constant-phase element related to the double layer capacitance, R_s is the ohmic resistance of the electrolyte solution, R_{ct} the charge-transfer resistance and W is the Warburg impedance (Z_w). These parameters can be calculated through the

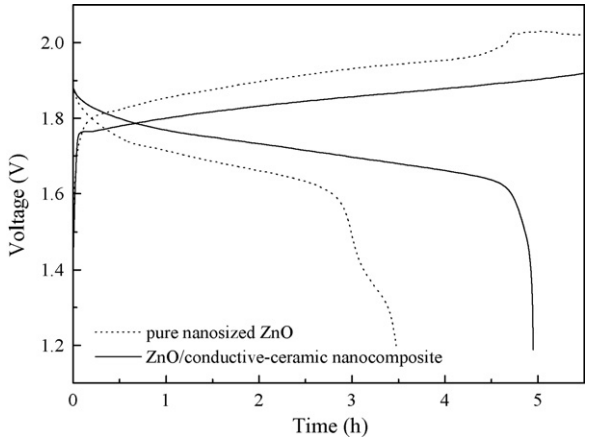

Fig. 4. Typical charge and discharge curves of Ni/Zn cells recorded at the 12th cycle.

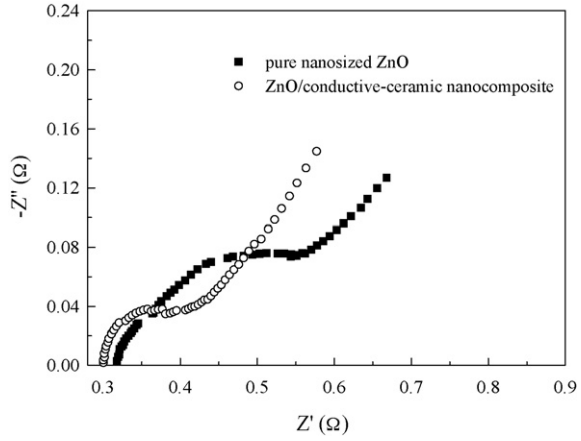

Fig. 6. Nyquist plots of the electrodes with the pure nanosized ZnO and ZnO/conductive-ceramic nanocomposite at 100% SOC.

Table 1
EIS parameters of the anodes for Ni/Zn rechargeable battery

Anode	Solution resistance, R_s (Ω)	Charge-transfer resistance, R_{ct} (Ω)	Capacitance of the double layer, Q_{dl} (F)
With pure ZnO	0.3177	0.2700	0.4286
With ZnO/conductive-ceramic	0.3003	0.1543	0.7393

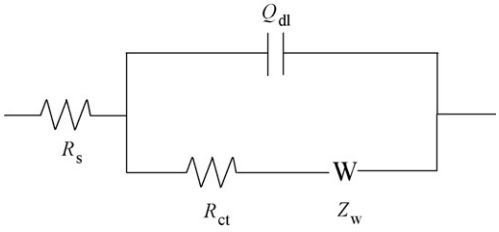

Fig. 7. Equivalent circuit model for electrochemical impedance measurements.

plots shown in Fig. 6 with ZSimpWin software. The values for the resistors and capacitor are listed in Table 1. It can be seen that the R_{ct} value of the pure nanosized ZnO is 0.27 Ω, much more than the R_{ct} value (0.1543 Ω) of the ZnO/conductive-ceramic electrode. A smaller charge-transfer resistance R_{ct} means that the electrochemical reaction occurring at the ZnO/conductive-ceramic electrode is easier, which results in a decrease in the electrochemical polarization of the electrode and an increase in the utilization of active material. As to the electrode structure, ZnO nanorods covering all the conductive ceramic destroy the compact pile-up of well-crystallized polyhedral ZnO crystals and increase the space within porous electrode, which can increase the passageways for OH^- and the actual reaction surface area of active material. The diffusion polarization of OH^- in the alkaline solution is dramatically decreased. Furthermore, the existence of conductive ceramic within the nanocomposite can lower the ohmic resistance of the electrode. The results show that the addition of conductive ceramic to the zinc electrode can reduce the electrochemical reaction impedance and enhance the electrochemical performance.

4. Conclusion

The ZnO/conductive-ceramic nanocomposite was prepared by a precipitation process and the synthesized ZnO nanorods were dispersed homogeneously on the surface of the conductive ceramic. Compared with pure nanosized ZnO, the ZnO/conductive-ceramic nanocomposite shows improved electrochemical properties, such as superior cycle stability, higher discharge capacity and utilization ratio, better electrochemical reactivity and reversibility of the electrode. The reasons for the improvement of electrochemical properties could lie in the three facts that (1) the conductive ceramic powders are used to form a highly conductive network, which helps to improve the electrical contact among ZnO particles and diminish the polarization of the electrode; (2) the structure of ZnO/conductive-ceramic nanocomposite increases the passageways for OH^- and actual reaction surface area of ZnO active material; and (3) the conductive ceramic becomes stable growth centers of Zn electrodeposits during charge/discharge processes, the morphology evolution of ZnO particles is suppressed. Therefore, the activity of ZnO is retained and the utilization of active material is also increased.

References

[1] F.R. McLarnon, E.J. Cairns, J. Electrochem. Soc. 138 (1991) 645.
[2] R.E.F. Einerhand, W. Visscher, J. Electrochem. Soc. 138 (1) (1991) 7.
[3] K. Bass, P.J. Mitchell, G.D. Wilcox, J. Smith, J. Smith, J. Power Sources 35 (1991) 333.
[4] J. Jindra, J. Power Sources 37 (1992) 297.
[5] J. McBreen, E. Gannon, Electrochim. Acta 26 (1981) 1439.
[6] J. McBreen, E. Gannon, J. Power Sources 15 (1985) 169.
[7] A. Renuka, A. Veluchamy, N. Venkatakrishnan, J. Appl. Electrochem. 22 (1992) 182.
[8] R. Shivkumar, G. Paruthimal Kalaigan, T. Vasudevan, J. Power Sources 75 (1998) 90.
[9] D. Coates, E. Ferreira, A. Charkey, J. Power Sources 65 (1997) 109.
[10] J.X. Yu, H. Yang, X.P. Ai, X.M. Zhu, J. Power Sources 103 (2001) 93.
[11] C.W. Lee, K. Sathiyanarayanan, S.W. Eom, H.S. Kim, M.S. Yun, J. Power Sources 159 (2006) 1474.
[12] C.J. Lan, C.Y. Lee, T.S. Chin, Electrochim. Acta 52 (2007) 5407.
[13] R. Renuka, S. Ramamurthy, K. Muralidharan, J. Power Sources 76 (1998) 197.
[14] R. Renuka, S. Ramamurthy, L. Srinivasan, J. Power Sources 89 (2000) 70.
[15] Y.F. Yuan, J.P. Tu, H.M. Wu, B. Zhang, X.H. Huang, X.B. Zhao, Electrochem. Commun. 8 (2006) 653.
[16] Y.F. Yuan, J.P. Tu, H.M. Wu, Y.Z. Yang, D.Q. Shi, X.B. Zhao, J. Power Sources 159 (2006) 357.
[17] Y. Zheng, J.M. Wang, H. Chen, J.Q. Zhang, C.N. Cao, Mater. Chem. Phys. 84 (2004) 99.
[18] Y.F. Yuan, J.P. Tu, H.M. Wu, Y.Z. Yang, D.Q. Shi, X.B. Zhao, Electrochim. Acta 51 (2006) 3632.
[19] M. Geng, D.O. Northwood, Int. J. Hydrogen Energy 28 (2003) 633.